Published in final edited form as:
Analyst. 2010 June ; 135(6): 1345–1350. doi:10.1039/c0an00028k.

Sensitive electrochemical immunosensor for matrix metalloproteinase-3 based on single-wall carbon nanotubes†

Bernard S. Munge[a], **Jacqueline Fisher**[a], **Lines N. Millord**[a], **Colleen E. Krause**[a], **Richard S. Dowd**[a], and **James F. Rusling**[b]

Bernard S. Munge: bernard.munge@salve.edu

[a] Salve Regina University, Department of Chemistry, Newport, Rhode Island, 02840-4192, USA; Fax: +1 401-341-2941; Tel: +1 401-341-3252

[b] Department of Chemistry, University of Connecticut, 55 North Eagleville Road, Storrs, CT, 06269-3060, USA

Abstract

A novel electrochemical immunosensor for the detection of matrix metalloproteinase-3 (MMP-3), a cancer biomarker protein, based on vertically aligned single-wall carbon nanotube (SWCNT) arrays is presented. Detection was based on a sandwich immunoassay consisting of horseradish peroxidase (14–16 labels) conjugated to a secondary antibody and/or a polymer bead loaded with multi-enzyme labels. Performance was optimized by effective minimization of non-specific binding (NSB) events using Bovine serum albumin (BSA), Tween-20 and optimization of the primary antibody and secondary antibody concentrations. Results provided a detection limit of 0.4 ng mL^{-1} (7.7 pM) for the 14–16 label sensor protocol and 4 pg mL^{-1} (77 fM) using a multiply enzyme labeled polymeric bead amplification strategy in 10 μL of calf serum. This immunosensor based on SWCNT arrays offers great promise for a rapid, simple, cost-effective method for clinical screening of cancer biomarkers for point-of-care diagnosis.

Introduction

Developing sensitive, reliable, accurate, low cost methods for detection of cancer protein biomarkers in complex biological matrixes is a major challenge, but with high payoff of future devices for early cancer screening and point-of-care diagnosis.[1–3] Such methods can also lead to a better understanding of the biochemistry of disease processes and in monitoring patient's responses to therapy.[4]

Various methods have been developed for protein measurement, including enzyme-linked immunosorbent assay (ELISA),[5–7] surface plasmon resonance (SPR),[8,9] magnetic bead-based electrochemiluminescence (ECL),[10] chemiluminescence,[11–14] fluorescence immunoassays,[15–17] mass spectrometry[18–20] and immuno-PCR.[21] Other methods such as nanowire transistors have shown excellent sensitivity for proteins binding to antibodies.[22,23] SPR, nanowire transistors, and impedance methods have enabled label free protein detection[24] and ELISA and ECL analyzers have found applications in research and hospital labs. At levels of current development, none of these approaches meets all criteria for point-of-care disease screening *via* detection of protein biomarkers in clinically relevant samples,

†Electronic supplementary information (ESI) available: immunosensor characterization and optimization. See DOI: 10.1039/c0an00028k

Correspondence to: Bernard S. Munge, bernard.munge@salve.edu.

which will require methods with high sensitivity, speed, and accuracy at low cost with minimal technical training of users.

Recently, we demonstrated a sensitive electrochemical SWCNT forest immunosensor for the detection of human cancer biomarker, prostate specific antigen (PSA) in serum and tissue lysate.[25,26] We used separate multiwall carbon nanotubes (MWCNTs) equipped with multiple enzyme labels and secondary antibodies to increase the number of enzyme labels per binding event for signal amplification. This approach provided a detection limit (DL) of 4 pg mL^{-1} for PSA in serum.[25] Alternatively, gold nanoparticle, AuNP, immunosensors fabricated from 5 nm glutathione–AuNPs for PSA in serum obtained by using ~1 μm magnetic nanoparticle–Ab_2–HRP bioconjugate with ~7500 HRPs per nanoparticle[27] gave a DL of 0.5 pg mL^{-1} (20 fM) PSA. Multilabel and single label approaches were combined with a 4-unit electrochemical immunoarray of single-wall carbon nanotube forest sensors to simultaneously measure four prostate cancer biomarkers in cancer patient serum.[28]

In this paper, we report a novel immunosensor amplification strategy for electrochemical detection of matrix metalloproteinase-3 (MMP-3), a cancer biomarker protein in clinically relevant calf serum samples for the first time. The MMP family of zinc-dependent endopeptidases represents a class of proteins that facilitates host and tumor communication.[29] Elevated expression of MMP-3 is associated with squamous cell carcinoma of the head and neck (SCCHN)[30] and adrenal tumors[31] and is a potential clinical tool for diagnosing and monitoring these diseases. Our protocol employs 500 nm diameter polymeric beads with multiple horseradish peroxidase (HRP) labels and secondary antibodies (Ab_2) attached to produce a giant molecular tag loaded with ~4200 enzyme labels (Scheme 1A). This provides a large signal amplification compared to 14–16 labels[32] per secondary antibody (Scheme 1B). This approach resulted in a detection limit of 4 pg mL^{-1} (77 fM) for MMP-3 in 10 μL undiluted calf serum.

Experimental

Chemicals and materials

Horseradish peroxidase (HRP, M_w 44 000), lyophilized 99% bovine serum albumin (BSA), Tween-20 and 2,2′-azino-bis-(3-ethylbenzthiazoline-6-sulfonic acid) (ABTS) were from Sigma/Aldrich. Polyclonal (Goat) primary anti-Human Matrix Metalloproteinase-3 (MMP-3) antibody (Ab_1), tracer secondary biotinylated anti-MMP-3 antibody (Ab_2), streptavidin modified HRP, and human MMP-3 standard in calf serum were from R&D systems. Single-walled carbon nanotubes (HiPco) were obtained from Carbon Nanotechnologies, Inc. Polystyrene microspheres (0.51 μm diameter) surface modified with streptavidin were from Bangs Laboratories, Inc. Immunoreagents were dissolved in pH = 7.0 phosphate buffered saline (PBS) (0.01 M phosphate, 0.14 M NaCl, 2.7 mM KCl) unless otherwise noted. 1-(3-(Dimethylamino)propyl)-3-ethylcarbodiimide hydrochloride (EDC) and *N*-hydroxysulfosuccinimide (NHSS) were dissolved in water immediately before use.

Fabrication of SWCNT immunosensors

SWCNT forests were fabricated and characterized as reported previously.[25,33] Briefly, purified, shortened, carboxyl-functionalized SWCNTs were dispersed in DMF, and aged at least one week. Ordinary basal plane pyrolytic graphite (PG) disks (A = 0.16 cm^2) with a thin layer of Nafion and $Fe(OH)_x$ were immersed in the aged SWCNT dispersions to form vertical SWCNTs forests, which were then dried in vacuum for 18 h.

For attachment of primary antibody, 30 μL of freshly prepared 400 mM EDC and 100 mM NHSS in water were placed onto the SWCNT forest electrodes, and washed off after 10 min. This was immediately followed by 3 h incubation at 37 °C with 20 μL of 200 ng mL^{-1} Ab_1

in pH 7.0 PBS buffer containing 0.1% Tween-20, a nonionic surfactant. The electrode was then washed with 0.1% Tween-20 and PBS buffer. The anti-MMP-3/SWNT electrode sensor constructed as described above was incubated for 1 h at 37 °C with 20 μL of 0.5% BSA + 0.1% Tween-20, followed by washing with 0.1% Tween-20 and PBS buffer for 3 minutes. Washing steps used here and during MMP-3 analysis were essential to block non-specific binding (NSB), and omission of any of the washing steps deteriorated sensitivity.

Preparation of the anti-MMP-3/HRP polystyrene bead bioconjugates

27 mg polystyrene beads coated with streptavidin (0.51 μm diameter) were put in a 1.5 mL centrifuge tube and washed twice with 100 μL pH = 7.0 PBS buffer by gentle shaking using an MCB 1200 biomagnetic processing platform for 1.0 min followed by ultra-centrifugation using a refrigerated Eppendorf centrifuge, 5417R at 13 000 rpm, 4 °C for 3.0 min. The supernatant was discarded and the resulting pellet redispersed in 36 μL pH = 7.0 PBS buffer by gentle vortexing using Cole-Parmer mixer, model 8891. In the homogeneous dispersion, biotinylated HRP and Ab_2 (anti-MMP-3) were added to a final concentration of 5 mg mL^{-1} and 1 μg mL^{-1} respectively. This was followed by 30 min incubation with gentle mixing using the MCB 1200 platform. The Ab_2–HRP coated polystyrene beads were then separated by ultra-centrifugation at 10 000 rpm, 4 °C for 3 min, the supernatant discarded and the resulting pellet redispersed and washed for 1 min using 200 μL pH = 7.0 PBS buffer containing 0.1% Tween-20. This step served to remove any free HRP and Ab_2 and was repeated 4 times. 200 μL of 0.1% Tween-20/PBS buffer was added to the bioconjugate precipitate, vortexed to form a homogenous dispersion (Ab_2–Polybead–HRP), stored at 4 °C, and then diluted in PBS/0.1% Tween-20 immediately before use. Bioconjugates were characterized by TEM and enzyme activity assays as described below.

Instrumentation

A CHI 660c electrochemical workstation was used for cyclic voltammetry and amperometry at ambient temperature (22 ±2 °C) in a three-electrode cell. Amperometry was done at −0.3 V *vs.* SCE with the SWCNT working electrode rotated at 2000 rpm, which gave optimum sensitivity. A Hitachi H-7000 TEM was used to characterize Ab_2–HRP polystyrene bead bioconjugates.

Immunosensor detection of MMP-3

Optimized steps in the assay procedure were as follows:

1. The immunosensor prepared as above was secured in an inverted position and incubated at 37 °C for 1 h 15 min with a 10 μL drop of serum containing MMP-3, followed by washing with 0.1% Tween-20 in buffer and then PBS buffer for 1.5 min each.
2. Next, the inverted sensor was incubated with 10 μL of 200 ng mL^{-1} biotinylated anti-MMP-3 antibody (Ab_2) in buffer containing 0.1% Tween-20 at 37 °C for 1 h 15 min, followed by incubation with 10 μL of streptavidin modified HRP or 10 μL of Ab_2–HRP polystyrene bead bioconjugate (85 pmol mL^{-1} in HRP) in buffer containing 0.1% Tween-20 at 37 °C for 1 h 15 minutes, followed by washing in 0.1% Tween-20 and PBS buffer for 3 min.
3. The immunosensor was then placed in an electrochemical cell containing 10 mL pH = 7.0 PBS buffer and 1 mM hydroquinone. Rotating disk amperometry at 2000 rpm was done at −0.3 V *vs.* SCE with injection of H_2O_2 to 0.4 mM to develop the amperometric signal.

Results

SWNT immunosensor using conventional Ab_2–HRP

We first established the optimum conditions for fabrication of the SWCNT arrays. The SWNT forest construction was optimized with the aid of Raman spectroscopy (see Fig. S1†) and Atomic Force Microscopy (AFM) (Scheme 1, inset). Raman spectra revealed high intensity bands corresponding to graphite (G) and defects (D) bands respectively. The D-bands typically observed between 1250 and 1450 cm^{-1}, originate from the first order scattering by in-plane hetero-atom substituents, grain boundaries, vacancies or the other defects and by finite size defects of the SWCNTs.[34] Fig. S1a† shows peaks at 230 cm^{-1}, characteristic of radial breathing mode (RBM) of SWCNT in the Nafion/$Fe(OH)_3$/SWCNT assembly confirming successful assembly of the SWCNT arrays, while this peak is absent in Nafion/$Fe(OH)_3$ (Fig. S1b†). The pH of the $FeCl_3$ solution plays a key role in the successful fabrication of SWCNT forests with the best SWCNT forest coverage, >98% at pH 1.7.[26] Scheme 1 (inset) shows AFM images of a SWCNT forest on flat silicon that confirming vertical orientation of the nanotubes in bundles of 20–100 nm diameter at coverages of >98% in agreement with previous reports.[25,33]

We constructed our immunoassay on the SWCNT array platform and optimized the experimental conditions for the electrochemical detection of MMP-3 in undiluted calf serum, previously shown to behave similarly to human serum in immunoassays.[25] The electrochemical detection follows a complex mechanism.[27] Scheme 2 illustrates the hydroquinone mediated electrochemical detection. H_2Q assists electron shuttling from the electrode to the oxidized HRP labels. In this catalytic mechanism, H_2O_2 oxidizes HRP to the ferryloxy radical form (eqn (2), Scheme 2) which is subsequently reduced to ferric HRP by H_2Q (eqn (3), Scheme 2). Quinone (Q) reduction at the electrode surface provides the measured immunosensor current signal. Both Q and ferric-HRP are regenerated in the catalytic pathway.

Inhibition of non-specific binding (NSB) was critical to achieve the best sensitivity and detection limits. Effective NSB blocking was achieved utilizing bovine serum albumin (BSA) and Tween-20. We also optimized the concentration of the capture antibody anti-MMP-3 (Ab_1) and the tracer secondary anti-MMP-3 anti-body (Ab_2) (see Experimental section).

Optimization experiments were done using 4 ng mL^{-1} MMP-3. Parameters optimized included the, Ab_2 diluents, washing strategies, concentration of BSA in the blocking step and concentrations of Ab_1 and Ab_2. These experiments were used to determine the most favorable conditions for the immunoassay. Initially, we used a PBS buffer solution containing 2% BSA + 0.05% Tween-20 as a diluent for the secondary antibody (Ab_2). Although BSA is often used to reduce non-specific binding in immunoassays,[35] research suggested that the presence of too much BSA in immunoassays might actually increase NSB.[36] We found 2% BSA produced significantly higher NSB (Fig. S2A†). Therefore, we opted to eliminate BSA from this step and use 0.1 M PBS + 0.05% T-20 as the diluent. The results produced a slightly greater difference between the controls and the samples (Fig. S2B†) (using 4 ng mL^{-1} MMP-3 for optimization). We also found that NSB was highly dependent on the efficiency of the washing steps.

A previous study showed accurate and replicable results when using wash buffers with slightly higher concentrations of Tween-20, and a blocking step with slightly lower

†Electronic supplementary information (ESI) available: immunosensor characterization and optimization. See DOI: 10.1039/c0an00028k

concentrations of BSA.[37] We tested the effect of this in our immunoassay by switching from 0.05% T-20 in our wash buffer to 0.1% T-20. We also changed our BSA concentration in the blocking step from 2% BSA to 0.5% BSA. This combination of changes seemed to have a significant effect on reducing NSB as seen by the decrease in the value of the controls and the standard deviations. The washing procedure was manipulated once more. In the original procedure the wash steps were performed by placing the electrodes into individual test tubes of wash buffer and manually and vigorously shaking the rack. We switched to washing the electrodes in beakers containing our wash buffers and a magnetic stirrer with spin-bars (with each electrode in a separate beaker). This method gave the lowest controls and provided the optimum signal difference between the sample and control signals (see Fig. S2C[†]).

The concentrations of the primary (capture) antibody, Ab_1, and the secondary (tracer) antibody, Ab_2, were optimized. For Ab_1, this was achieved by varying the concentration used to link Ab_1 to the sensor surface, then doing the complete immunoassay while keeping the MMP-3 and Ab_2 concentrations at 4 ng mL^{-1} and 200 ng mL^{-1} respectively. At the same time, control experiments were done without antigen present (Fig. 1A). Our results showed the smallest NSB at lower concentrations of Ab_1. In particular the largest difference between the control and sample signals occurred at 200 ng mL^{-1} Ab_1 (Fig. 1A). Therefore, this was chosen as the optimum concentration of Ab_1. The concentration of Ab_2 was optimized in a similar manner, keeping the concentration of Ab_1 constant at 200 ng mL^{-1} (optimum). This experiment showed controls lower than the sample at 200 ng mL^{-1} and 2000 ng mL^{-1} Ab_2 concentration (Fig. 1B). We chose 200 ng mL^{-1} Ab_2 as optimum concentration because it produced the largest signal difference coupled with lower controls. These optimal conditions of 200 ng mL^{-1} for Ab_1 and Ab_2 were used in procedures to detect various amounts of MMP-3 in calf serum. In the optimized procedure, immunosensors were first incubated for 1 h with 20 μL 0.5% BSA + 0.1% Tween-20, then washed with 0.1% Tween-20 in buffer. After attachment of Ab_1, 10 μL of undiluted calf serum containing MMP-3 were incubated on the inverted sensor surface, blocking buffer was used to wash, then the sensor was incubated with 10 μL biotinylated secondary anti-MMP-3 followed with streptavidin–HRP label giving 14–16 labels per Ab_2.[32] The washed immunosensor was then placed into an electrochemical cell containing the mediator hydroquinone in buffer, and hydrogen peroxide was injected for signal development (Fig. 2A).

The steady state current increased linearly (Fig. 2B) with log MMP-3 concentration from 0.4 to 40 ng mL^{-1} with a sensitivity of 77.6 nA/log [MMP-3]. Device-to-device reproducibility is illustrated by the small error bars with a relative standard deviation (RSD) of 9%. The detection limit of 0.4 ng mL^{-1} was estimated as the zero MMP-3 control signal plus three-times the control noise level (Fig. 2A). Results indicate that using BSA and optimum detergent concentration for NSB blocking, washing procedure and optimizing the concentration of Ab_1 and Ab_2 are very effective to minimize NSB in serum. Control experiment in Fig. 2A represents a SWCNT immunosensor taken through the full procedure without exposure to MMP-3, and the response reflects the sum of residual NSB and direct reduction of hydrogen peroxide.

Ab_2–HRP polymeric beads bioconjugates

Multiple HRP labels were attached to polystyrene (0.51 μm) microsphere beads for multilabel amplification[21,38,39] to enhance sensitivity. Our approach was to link HRP and Ab_2 to streptavidin coated polystyrene microspheres with a reaction mixture having a 200/1 HRP/Ab_2 molar ratio. The mutilabel particles were used in place of the conventional Ab_2–HRP(14–16) complex.

Ab_2 and HRP were simultaneously attached to the polystyrene microspheres by the streptavidin–biotin interaction, one of the binding interactions in nature ($K_a = 10^{15}$ M^{-1} *vs.* 10^7–10^{11} M^{-1} for antibody–antigen interactions).[40]

Transmission electron microscopy (TEM) images show the derivatized polymeric beads with fuzzy features (Fig. S3B†) when compared to the underivatized beads (Fig. S3A†) suggesting successful immobilization of HRP. To determine the amount of active HRP per unit weight of microsphere, the Ab_2–Polybead–HRP dispersion was reacted with HRP substrate 2,2′-azino-bis-(3-ethylbenzthiazoline-6-sulfonic acid) (ABTS)[41] and H_2O_2. The reaction produces a soluble product with characteristic optical absorbance at 405 nm. A linear increase in absorbance of the product at 405 nm (Fig. 3) was found, and the slope was used to estimate[42] an HRP activity of 92 Units mL^{-1} of undiluted Ab_2–Polybead–HRP. This was compared to a standard curve constructed with underivatized HRP, after subtracting the background absorbance of an equivalent dispersion of underivatized polymer beads.

The concentration of active HRP in the stock Ab_2–Polybead–HRP dispersion was determined in this way to be 3.77 μg mL^{-1}. Considering 27 mg of microspheres used to prepare the Ab_2–Polybead–HRP conjugate, we had 0.9 pmol HRP per mg beads or 85 pmol HRP mL^{-1} of dispersion. Using the manufacturer's specifications for the microspheres with 0.51 μm diameters and a density of 1.359×10^{11} microspheres per mL, the number of active HRP was estimated as 4168 per microsphere.

Similar NSB blocking protocols as summarized for Ab_2–HRP were followed when using the Ab_2–Polybead–HRP bioconjugate (Scheme 1A) to measure response of the SWCNT immunosensor to MMP-3. Optimization of bioconjugate concentration, a major factor in minimizing NSB, was done by evaluating the performance of dilutions of the stock Ab_2–Polybead–HRP using 0.1% Tween-20. 85 pmol HRP mL^{-1} gave the best detection limit. BSA was not used in the dilution as it was found to deteriorate the detection limit.

Fig. 4A shows the amperometric detection of MMP-3 in undiluted calf serum using the Ab_2–HRP–polymeric bead conjugate with the SWCNT immunosensors. Signal intensity was greatly increased for this amplified system compared to the conventional Ab_2–HRP (*cf.* Fig. 2A). The Ab_2–Polybead–HRP gave a linear calibration curve for log MMP-3 concentration in calf serum from 4–300 pg mL^{-1}. Device-to-device reproducibility is illustrated by the small error bars with a relative standard deviation (RSD) of 10%. Sensitivity as the slope of the calibration graph (Fig. 4B) at low concentration range was 4250 nA/log [MMP-3]. These results show 55-fold higher sensitivity for multilabel Ab_2–Polybead–HRP than Ab_2–HRP(14–16), with an estimated detection limit of 4 pg mL^{-1} based on 3 times the average noise above the zero MMP-3 control in a 10 μL sample. This detection limit is similar to our recent results for PSA detection using an Ab_2–CNT–HRP bioconjugate[25] for signal amplification. However, the polymeric beads amplification strategy offers over 65-fold higher sensitivity.

Discussion

Results described above show that SWCNT immunosensors can be used to detect MMP-3 cancer biomarkers in complex biological samples with high sensitivity and selectivity (Fig. 2 and 4). Further, the immunosensors have a very good reproducibility as demonstrated by device-to-device standard deviations. The best sensitivity is obtained using the Ab_2–Polybead–HRP bioconjugates with high enzyme label/Ab_2 ratios for signal amplification. The success of this novel signal amplification strategy also depends on minimizing the nonspecific binding (NSB) of the secondary antibody material, which commonly controls the detection limit of sandwich immunoassays.[43,44] NSB was effectively controlled by using

BSA and Tween-20 in blocking buffers at optimized concentrations, providing an estimated sensitivity to MMP-3 at concentrations as low as 4 pg mL^{-1} in only 10 μL of undiluted calf serum (Fig. 4). This DL is lower than normal serum MMP-3 levels for patients with cancer. For example, patients with adrenal cortex carcinoma had a mean value of 127 ng mL^{-1} compared to 16 ng mL^{-1} in control group.[31]

The high sensitivity of the SWCNT immunosensors using the Ab_2–Polybead–HRP bioconjugates is correlated to several factors including (a) several thousands of labels per binding event provided by using Ab_2–Polybead–HRP bioconjugates in place of conventional Ab_2–HRP; (b) SWCNT forest properties including excellent conductivity and high surface area that provide a high density of primary antibodies, and (c) the catalytic nature of the enzyme label, in which HRP is activated by hydrogen peroxide to a ferryloxy form of the enzyme that is electrochemically reduced in a catalytic cycle.[45]

These results suggest an excellent potential for array fabrication leading to real time multiplexed cancer biomarker detection, an exciting possibility for early cancer detection and monitoring that we are currently exploring. Immobilization of electroactive enzyme labels at the sensing element is a viable approach for sensor array fabrication as it minimizes electrochemical crosstalk between array elements, while enzymes producing a soluble electroactive product place specific restrictions on array design.[46,47]

Conclusions

We have demonstrated highly sensitive and selective SWCNT electrochemical sensor for the detection of MMP-3, an emerging cancer biomarker protein, in calf serum as a clinically related medium. A multilabeled polymeric bead amplification strategy gave a ultralow detection limit of 4 pg mL^{-1} (77 amol mL^{-1}) in the 10 μL serum sample which is comparable to carbon nanotube amplification for PSA detection,[25] with over 65-fold better sensitivity compared to a single labeled Ab_2. SWCNT immunosensors in conjunction with multilabel amplification show great potential as components in future cancer diagnostics.

Supplementary Material

Refer to Web version on PubMed Central for supplementary material.

Acknowledgments

This research was financially supported by Grant number P20RR016457 awarded to BSM by the National Center for Research Resource (NCRR) a component of NIH and in part by US PHS grant ES013557 awarded to JFR from National Institutes of Environmental Health Sciences of NIH. Its contents are solely the responsibility of the authors and do not necessarily represent the official views of NCRR or NIH.

References

1. Kitano H. Science 2002;295:1662. [PubMed: 11872829]
2. Figeys D. Anal Chem 2003;75:2891. [PubMed: 12945794]
3. Hood E. Environ Health Perspect 2003;111:A817.
4. Xiao Z, Prieto D, Conrads TP, Veenstra TD, Isaaq HJ. Mol Cell Endocrinol 2005;230:95–106. [PubMed: 15664456]
5. Yates AM, Elvin SJ, Williamson DE. J Immunoassay 1999;20:31. [PubMed: 10225513]
6. Christiansen M, Hogdall CK, Anderson JR, Norgaard-Perdersen B. Scand J Clin Lab Invest 2001;61:205. [PubMed: 11386607]
7. Ju HX, Yan G, Chen F, Chen HY. Electroanalysis (N Y) 1999;11:124.
8. Yu F, Persson B, Lofas S, Knoll W. Anal Chem 2004;76:6765. [PubMed: 15538801]

9. Lee HJ, Wark AW, Corn RM. Analyst 2008;133:975. [PubMed: 18645635]
10. Debad, JB.; Glezer, EN.; Leland, JK.; Sigal, GB.; Wholstadter, J. Electrogenerated Chemiluminescence. Bard, AJ., editor. Marcel Dekker; NY: 2004. p. 359
11. Lin J, Yan F, Ju HX. Appl Biochem Biotechnol 2004;117:93. [PubMed: 15159553]
12. Fu Z, Hao C, Fei X, Ju HX. J Immunol Methods 2006;312:61. [PubMed: 16647079]
13. Zhang Q, Wang X, Li Z, Lin J. Anal Chim Acta 2009;631:212. [PubMed: 19084628]
14. Zheng Y, Chen H, Liu X, Jiang J, Luo Y, Shen G, Yu R. Talanta 2008;77:809.
15. Cui R, Pan H, Zhu J, Chen H. Anal Chem 2007;79:8494. [PubMed: 17927140]
16. Matsuya T, Tashiro S, Hoshino N, Shibata N, Nagasaki Y, Kataoka K. Anal Chem 2003;75:6124. [PubMed: 14615991]
17. Song SP, Li B, Hu J, Li MQ. Anal Chim Acta 2004;510:147.
18. Ishii A, Seno H, Watabe-Suzuki K, Kumazawa T, Matsushima H, Suzuki O, Katsumata Y. Anal Chem 2000;72:404. [PubMed: 10658337]
19. Niederkofler EE, Tubbs KA, Gruber K, Nedelkov D, Kiernan UA, Williams P, Nelson RW. Anal Chem 2001;73:3294. [PubMed: 11476228]
20. Hu SH, Zhang SC, Hu ZC, Xing Z, Zhang XR. Anal Chem 2007;79:923. [PubMed: 17263317]
21. Saito K, Kobayashi D, Sasaki M, Araake H, Kida T, Yagihashi A, Yajima T, Kameshima H, Wanatabe N. Clin Chem (Washington, D C) 1999;45:665.
22. (a) Patolsky F, Zheng G, Lieber CM. Anal Chem 2006;78:4260. [PubMed: 16856252] (b) Zhang H, Zhao Q, Li XF, Le XC. Analyst 2007;132:724. [PubMed: 17646870]
23. Kim S, Rusling JF, Papadimitrakopolous F. Adv Mater 2007;19:3214. [PubMed: 18846263]
24. Tkac, J.; Davis, JJ. Label-free field effect protein sensing. In: Davis, JJ., editor. Engineering the Bioelectronic Interface. Royal Soc. Chem; UK: 2009. p. 193-224.
25. Yu X, Munge B, Patel V, Jensen G, Bhirde A, Gong JD, Kim SN, Gillespie J, Gutkind JS, Papadimitrakopoulos F, Rusling JF. J Am Chem Soc 2006;128:11199. [PubMed: 16925438]
26. Rusling, JF.; Yu, X.; Munge, BS.; Kim, SN.; Papadimitrakopoulos, F. Engineering the Bioelectronic Interface. Davis, JJ., editor. Royal Soc. Chem; UK: 2009. p. 94-118.
27. Kim S-N, Rusling JF, Papadimitrakopolous F. Carbon nanotubes in electronic and electrochemical detection of biomolecules. Adv Mater 2007;19:3214. [PubMed: 18846263]
28. Chikkaveeriah BV, Bhirde A, Malhotra R, Patel V, Gutkind JS, Rusling JF. Anal Chem 2009;81:9129. [PubMed: 19775154]
29. McCawley LJ, Crawford HC, King LE Jr, Mudgett J, Matrisian LM. Cancer Res 2004;64:6965. [PubMed: 15466188]
30. Linkov F, Lisovich A, Yurkovetsky Z, Marrangoni A, Velikokhatnaya L, Nolen B, Winans M, Bigbee W, Siegfried J, Lokshin A, Ferris RL. Cancer Epidemiol Biomarkers Prev 2007;16:102. [PubMed: 17220337]
31. Kolomecki K, Stepien H, Bartos M, Kuszak K. Endocr Regul 2001;35:9. [PubMed: 11308991]
32. Munge BS, Krause CE, Malhotra R, Patel V, Gutkind JS, Rusling JF. Electrochem Commun 2009;11:1009. [PubMed: 20046945]
33. Chattopadhyay D, Galeska I, Papadimitrakopoulos F. J Am Chem Soc 2001;123:9451. [PubMed: 11562232]
34. Eklund PC. Adv Phys 2000;49:705.
35. Veetil JV, Ye K. Biotechnol Prog 2007;23:517. [PubMed: 17458980]
36. Brogan KL, Shin JH, Schoenfisch MH. Langmuir 2004;20:9729. [PubMed: 15491208]
37. Wang J, Liu G, Engelhard MH, Lin Y. Anal Chem 2006;78:6974. [PubMed: 17007523]
38. Wang J. Small 2005;1:1036. [PubMed: 17193390]
39. Munge B, Liu G, Collins G, Wang J. Anal Chem 2005;77:4662. [PubMed: 16013886]
40. Hoshi T, Anzai J, Osa T. Anal Chem 1995;64:770. [PubMed: 7702192]
41. Matsuda H, Tanaka H, Blas BL, Nosenas JS, Tokawa T, Ohsawa S. Jpn J Exp Med 1984;54:131. [PubMed: 6542945]

42. Jensen GC, Yu X, Gong JD, Munge B, Bhirde A, Kim SN, Papadimitrakopoulos F, Rusling JF. J Nanosci Nanotechnol 2009;9:249. [PubMed: 19441303]

43. Wilson DS, Nock S. Angew Chem, Int Ed 2003;42:494.

44. Ward AM, Catto JWF, Hamdy FC. Ann Clin Biochem 2001;38:633. [PubMed: 11732646]

45. Ruzgas, T.; Lindgren, A.; Gorton, L.; Hecht, H-J.; Reichelt, J.; Bilitewski, U. Electroanalytical Methods for Biological Materials. Chambers, JQ.; Bratjer-Toth, A., editors. Marcel Dekker; New York: 2002. p. 233

46. Kojima K, Hiratsuka A, Suzuki H, Yano K, Ikebukuro K, Karube I. Anal Chem 2003;75:1116. [PubMed: 12641231]

47. Wilson MS. Anal Chem 2005;77:1496. [PubMed: 15732936]

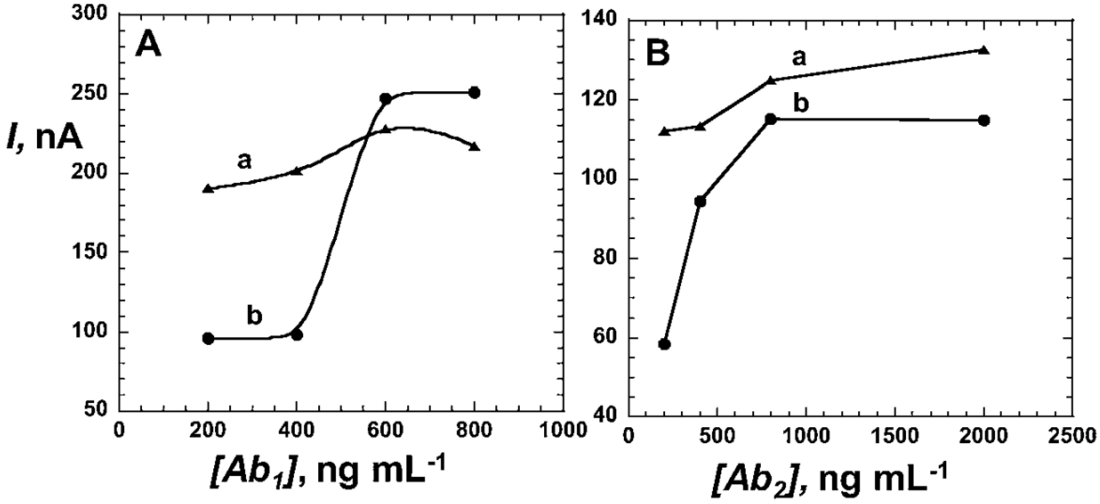

Fig. 1.

Optimization of (A) the primary antibody, anti-MMP-3 (Ab_1) and (B) the secondary antibody, anti-MMP-3 (Ab_2) concentrations; (a) the complete immunoassay using 4.0 ng mL^{-1} MMP-3 concentration and (b) controls with 0 ng mL^{-1} MMP-3. In (A), the secondary antibody, Ab_2 (tracer), concentration was kept fixed at 200 ng mL^{-1} in both the controls and the samples while in (B), the optimum Ab_1 (200 ng mL^{-1}) concentration was used to optimize Ab_2 concentration.

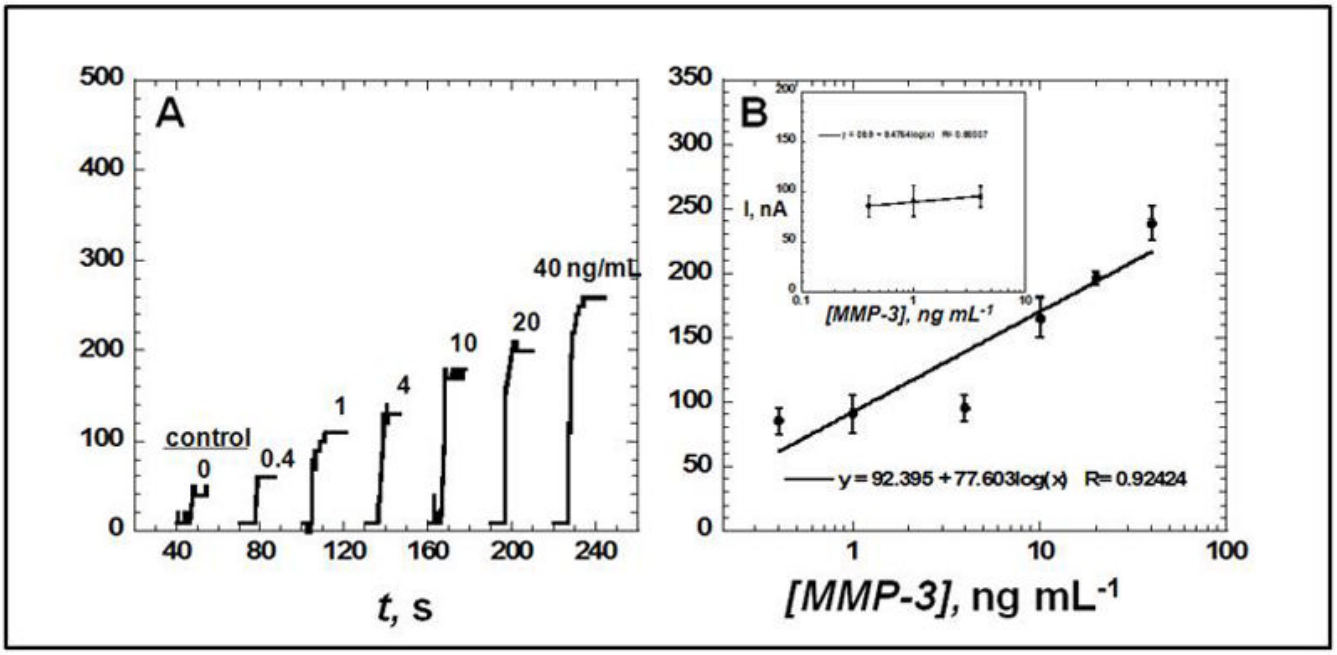

Fig. 2.

Amperometric response for SWCNT immunosensors incubated with MMP-3 (concentration in ng mL^{-1} labeled on curves) in 10 μL of undiluted newborn calf serum for 1.25 hours, then (A) followed by 10 μL of 200 ng mL^{-1} biotin–Ab_2 in 0.1% Tween-20 for 1.25 h, then 10 μL of streptavidin modified HRP for 30 min, showing current at −0.3 V and 2000 rpm after placing electrodes in buffer containing 1 mM hydroquinone mediator, then injecting H_2O_2 to 0.4 mM to develop the signal. Controls shown on right with MMP-3 concentrations: full SWCNT immunosensor with 0 ng mL^{-1} MMP-3 and (B) influence of log MMP-3 concentration on steady state amperometric current for SWNT immunosensor using anti-MMP-3–HRP(14–16). Error bars in part B represent device-to-device standard deviations (n = 3).

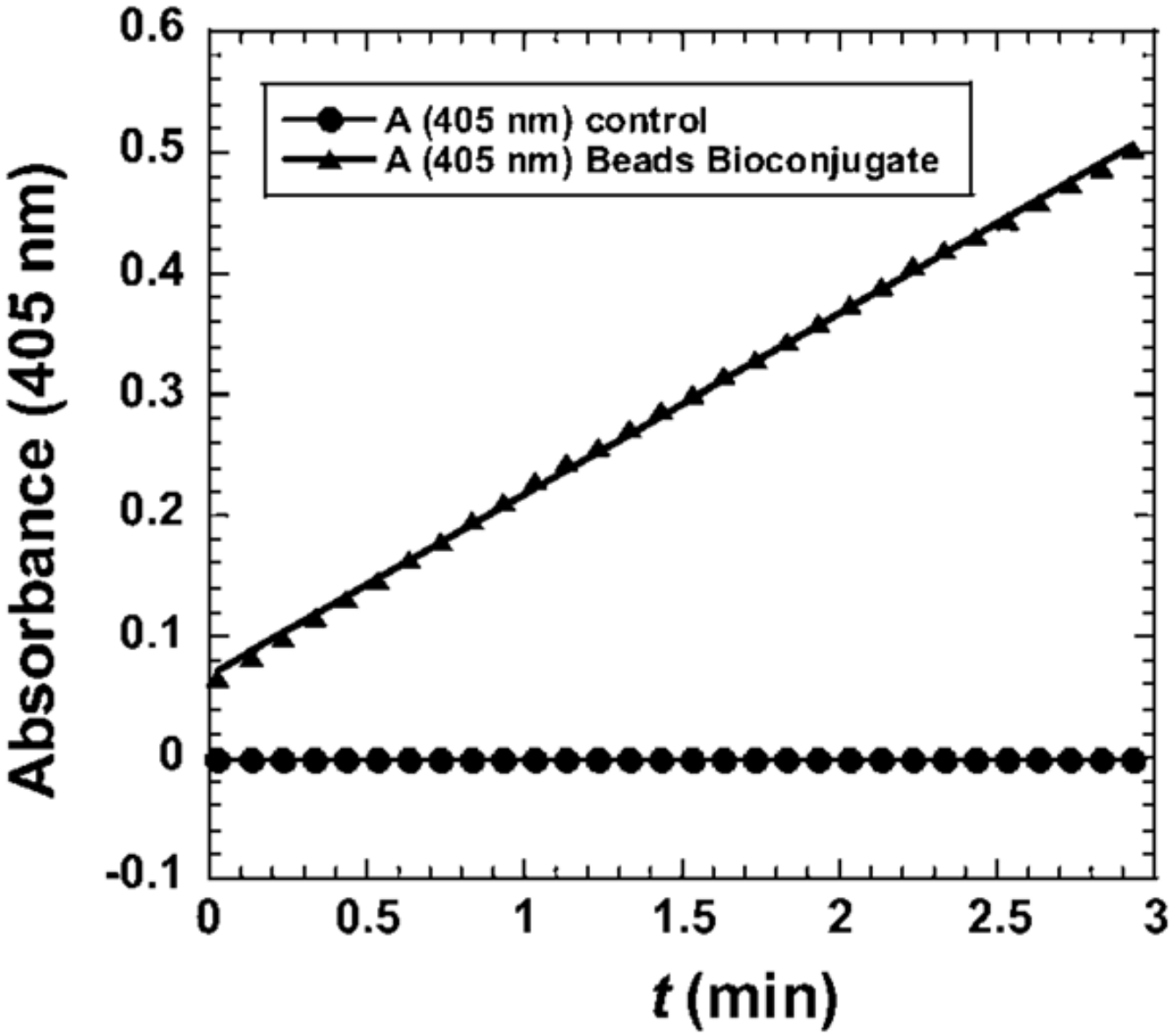

Fig. 3.
Results of enzyme activity assay of HRP–Polybead–Ab_2 bioconjugate activated by H_2O_2 with ABTS as substrate to give colored product with absorbance at 405 nm.

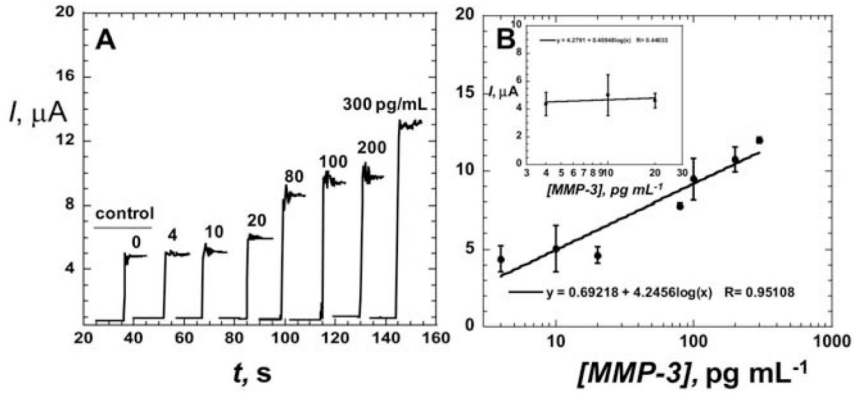

Fig. 4.

Amperometric response for SWCNT immunosensors incubated with MMP-3 (concentration in pg mL^{-1} labeled on curves) in 10 μL of undiluted newborn calf serum for 1.25 h: (A) current at −0.3 V and 2000 rpm using the Ab_2–HRP polymeric beads bioconjugate. Controls shown on left with MMP-3 concentrations: full SWCNT immunosensor with 0 pg mL^{-1} MMP-3. (B) Influence of log MMP-3 concentration on steady state current for immunosensor using Ab_2–Polybead–HRP bioconjugate. Error bars in part B represent device-to-device standard deviations (n = 3).

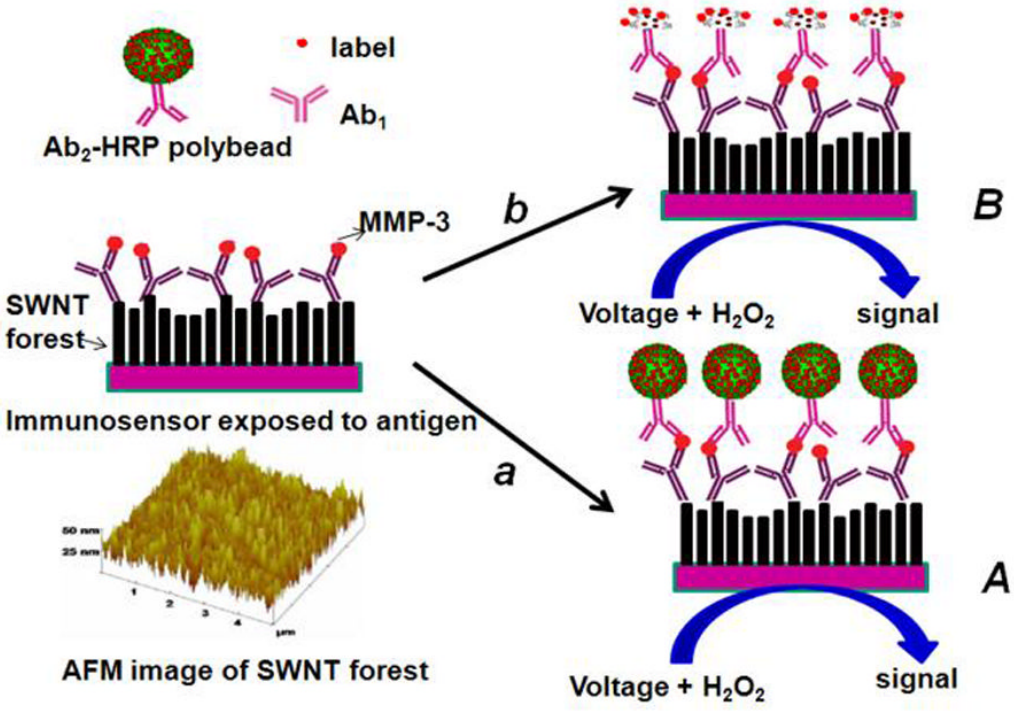

Scheme 1.

Illustration of detection principles of SWCNT immunosensors. On the bottom left is a tapping mode atomic force microscope image of a SWCNT forest that serves as the immunosensor platform. On the right is a cartoon of a SWCNT immunosensor platform used for capture antibody (Ab_1) bioconjugation and subsequent antibody–antigen sandwich immunoassay (HRP is the enzyme label). Picture (A) on the right shows the immunosensor after treating with Ab_2–Polybead–HRP to obtain amplification by providing numerous enzyme labels per binding event. Picture (B) on the right shows the immunosensor after treating with a conventional HRP–Ab_2 (biotinylated Ab_2 followed by streptavidin modified HRP) providing 14–16 labels per binding event. The final detection step involves immersing the immunosensor after secondary antibody attachment into a buffer containing mediator in an electrochemical cell, applying voltage, and injecting a small amount of hydrogen peroxide.

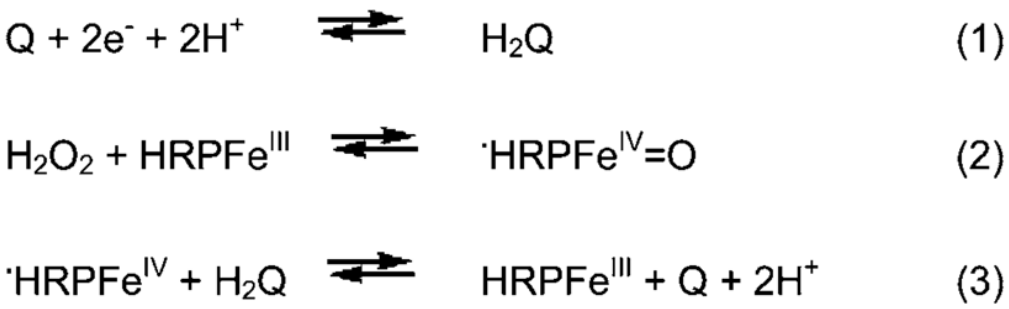

Scheme 2.
Postulated catalytic mechanism for mediated electrochemical detection of HRP labels.